Stability Analysis of Load Frequency Control Systems with Sampling and Transmission Delay

Haocheng Luo, *Student Member, IEEE*, Ian A. Hiskens, *Fellow, IEEE*, Zechun Hu, *Senior Member, IEEE*

***Abstract*—To analyze the delay-dependent stability of a load frequency control (LFC) system with transmission delays, the continuous-time model with delay is usually adopted. However, practical LFC is actually a sampled-data system, where the power commands sent to generation units are updated every few seconds. It is therefore desirable to analyze the delay-dependent stability of LFC when sampling is introduced. This paper undertakes stability analysis of LFC with both sampling and transmission delay. The model of the LFC system is first modified to consider sampling and transmission delay separately. Based on Lyapunov stability theory and linear matrix inequalities, a new stability criterion for linear systems with both sampling and transmission delay is proposed using the Wirtinger-based integral inequality and its affine version. The proposed criterion is applicable for both time-invariant and time-varying transmission delays. Case studies are undertaken on both single-area and two-area LFC systems to verify the effectiveness and advantage of the proposed method.**

***Index Terms*—Load frequency control, delay-dependent stability, delay margin, sampled-data systems, transmission delay.**

NOMENCLATURE

Sets

$\mathbb{R}^+$	set of positive scalars
$\mathbb{R}^{n\times m}$	set of $n \times m$ real matrices
$\mathbb{S}^n$	set of $n \times n$ symmetric matrices
$\mathbb{S}^n_+$	set of $n \times n$ symmetric and positive definite matrices

Variables

ACE_i	area control error (ACE) of the i-th control area
Δf_i	frequency deviation of the i-th control area
$\Delta P_{m,i}$	deviation in generator mechanical power output of the i-th control area
$\Delta P_{v,i}$	deviation in turbine valve position of the i-th control area
$\Delta P_{d,i}$	load change in the i-th control area
$\Delta P_{tie,i}$	deviation in tie-line power exchange of the i-th control area
$\tau_i(t)$	transmission delay of the i-th control area

Parameters

M_i	inertia constant of the i-th control area
D_i	damping constant of the i-th control area
$T_{ch,i}$	time constant of turbine of the i-th control area
$T_{g,i}$	time constant of governor of the i-th control area
R_i	speed droop of the i-th control area
β_i	frequency bias factor of the i-th control area
T_{ij}	synchronizing torque coefficient between the i-th and j-th control areas
$K_{P,i}$	proportional gain of the PI controller in the i-th control area
$K_{I,i}$	integral gain of the PI controller in the i-th control area

Other Notation

$A \succ 0$	A is symmetric and positive definite
A^T	matrix transposition of A
$\mathrm{diag}(A, B)$	block-diagonal matrix formed from A and B, i.e., $\mathrm{diag}(A,B) = \begin{bmatrix} A & 0 \\ 0 & B \end{bmatrix}$
$\mathrm{He}(A)$	sum of A and its transposition, i.e., $\mathrm{He}(A) = A + A^T$
I_n	identity matrix of size n
$0_{n\times m}$	zero matrix of size $n \times m$

I. INTRODUCTION

STABILITY and performance of load frequency control (LFC) are crucial for secure and economic operation of power systems. The effectiveness of LFC is affected by many factors, including time delays in the communication network. Transmission delays are often ignored in LFC stability analysis and controller design when dedicated communication networks are employed to transmit measurements and broadcast control signals, though a constant transmission delay exists. However, future LFC systems may use open communication networks, in which case transmission delays will inevitably arise [1]–[4]. Furthermore, transmission delays may vary randomly due to factors such as communication protocols, network loading, and routing over different types of communication lines. For instance, the simulation results in [5] showed that the time delays in LFC systems can vary in the interval [0.15, 2] seconds when an open network is used. To incorporate a large number of distributed energy resources into LFC systems, multi-layer communication networks are needed. In such multi-layer networks, various kinds of delays, due to communications, signal processing, decision making and

This work was partially supported by National Key Research and Development Program of China (2016YFB0900500). *(Corresponding author: Zechun Hu.)*

H. Luo and Z. Hu are with the Department of Electrical Engineering, Tsinghua University, Beijing, 100084, P. R. China (email: luohc15@mails.tsinghua.edu.cn; zechhu@tsinghua.edu.cn).

I. A. Hiskens is with the Department of Electrical Engineering and Computer Science, University of Michigan, Ann Arbor, MI, 48104, USA (email: hiskens@umich.edu).

network transition, exist in every layer and should be summed to give the total delay from the control center to the regulation resources. The field tests in [6] showed that time delays are around 3 seconds when a multi-layer communication network is used for frequency control. Such delays can degrade the regulation performance of LFC and even threaten stability [2], [7], [8]. Hence, stability analysis of LFC in the presence of transmission delays is of increasing importance.

The objective of the proposed stability analysis is to determine the maximal allowable transmission delay such that stability is maintained. Two approaches are generally used to estimate the maximal allowable delay of a time-delay system. The frequency-domain direct method utilizes the well-known condition that a closed-loop system is asymptotically stable if all the roots of its characteristic equation lie in the open left-half plane. In [4], the delay margins of LFC systems are calculated using the Schur-Cohn algorithm. The authors of [9], [10] propose two direct and exact methods to determine the delay margin of LFC by transforming the transcendental characteristic equation into regular polynomials. The delay margin results provided by these methods are very accurate, but are limited to continuous systems with a constant delay. Other recent studies have used frequency-domain methods to analyze power systems with multiple time-varying delays [11], [12], but their assumptions and approximations prevent them from providing exact delay margins.

The alternative time-domain indirect approach utilizes Lyapunov stability theory and linear matrix inequalities (LMIs) to estimate the delay margin. In [13], the time-domain approach is used for delay-dependent stability analysis of LFC with constant or time-varying delays, and the relationship between delay margins and controller gains is investigated. A further study is provided in [14] to show interactions of the delay margins of different control areas for deregulated LFC systems. This study also provides a guide to considering delay margins in LFC controller design. To reduce the conservativeness of the delay margin estimation, [15], [16] propose two stability criteria; one uses an infinite-series-based inequality and the other the second-order Bessel-Legendre inequality. Each inequality is used together with a reciprocally convex combination inequality to bound the integral terms in the time derivative of the Lyapunov-Krasovskii functional. The effect of electric vehicle participation on the stability of LFC is considered in [17], where a delay-dependent stability criterion for a linear system with multiple time-varying delays is proposed.

Although the time-domain method unavoidably introduces some conservativeness, its ability to handle both time-invariant and time-varying delays is still attractive. Furthermore, the LMI-based criterion can also be used to design robust LFC controllers that ensure delay-dependent stability and provide satisfactory regulating performance, extending the application of such time-domain indirect methods [18].

Practical LFC is a sampled-data system, i.e., the LFC controller updates the power commands sent to generation units every 2 to 4 seconds [19], [20]. The stability of a time-delay system can be significantly affected by sampling [21]–[23]. However, most investigations of delay-dependent stability of LFC systems have not considered sampling. A brief discussion is provided in [14] on the use of delay margin results to guide the selection of the sampling interval of an LFC controller. However, [14] treats sampling-induced delay as a general input delay. Such an approach neglects the sawtooth-like characteristic of sampling-induced delay and hence gives conservative results. Consequently, stability analysis of LFC systems with both sampling and transmission delay requires further investigation.

This paper addresses delay-dependent stability of sampled-data LFC systems. Sampling effects are carefully considered in both modeling and stability criterion derivation. The LFC system is first modeled in a way that separately considers transmission delay and sampling. This model facilitates investigation of their differing effects on stability. Based on [24] and [25], a new stability criterion for linear systems with both sampling and transmission delay is proposed. For various values of the proportion-integral (PI) gains, this new method is used to compute the delay margins of the LFC system with both time-invariant and time-varying transmission delays. These results are compared with those obtained using the analysis methods of [13], [26]. Time-domain simulation of the LFC system is undertaken to verify the effectiveness of the proposed method. Discussion also covers the effects of sampling intervals and ACE filtering, incorporating battery storage systems (BSSs), and use of the delay margin results to guide LFC design.

The remainder of the paper is organized as follows. Section II presents the LFC system model with both sampling and transmission delay. Section III develops a delay-dependent stability criterion for linear systems with sampling and delay, along with the method to implement this criterion to calculate delay margins. Case studies for various system settings are provided in Section IV. Section V presents conclusions.

II. Modeling Load Frequency Control with Sampling and Delay

Steady-state or small-disturbance stability analysis requires a state-space model of LFC linearized around an equilibrium point [8], [27]. Incorporating sampling and delay in the control system requires some modification to the conventional model of the LFC system. This section develops the required extensions to the LFC system model, with sampling and delay considered separately rather than aggregated into a single quantity.

The block diagram of the i-th control area in a multi-area LFC system of N control areas is shown in Fig. 1. Before undertaking the detailed derivation, several aspects of the model are worth noting:

1) Although transmission delays exist in many parts of an LFC system, e.g., from remote terminal units (RTUs) to control center and from control center to individual generation units, all delays are aggregated into a single time-invariant or time-varying delay per control area [13]–[17], [26], [28]. This is shown in Fig. 1.
2) The LFC model includes an equivalent model of a non-reheat steam generation unit, but it can be extended to

include multiple types of turbines, such as reheat steam units and hydraulic units.

3) A PI controller is used in the LFC system model.

The dynamic model of the multi-area LFC system can be expressed as [8], [27]:

$$\begin{aligned} \dot{x}(t) &= Ax(t) + Bu(t) + F\Delta P_d, \\ y(t) &= Cx(t), \end{aligned} \tag{1}$$

where

$$\begin{aligned} x_i(t) &= [\Delta f_i \quad \Delta P_{m,i} \quad \Delta P_{v,i} \quad \int ACE_i \quad \Delta P_{tie,i}]^T, \\ y_i(t) &= [ACE_i \quad \int ACE_i]^T, \\ x(t) &= [x_1(t) \quad x_2(t) \quad \cdots \quad x_N(t)]^T, \\ y(t) &= [y_1(t) \quad y_2(t) \quad \cdots \quad y_N(t)]^T, \\ u(t) &= [u_1(t) \quad u_2(t) \quad \cdots \quad u_N(t)]^T, \\ \Delta P_d &= [\Delta P_{d,1} \quad \Delta P_{d,2} \quad \cdots \quad \Delta P_{d,N}]^T, \\ A &= \begin{bmatrix} A_{11} & A_{12} & \cdots & A_{1N} \\ A_{21} & A_{22} & \cdots & A_{2N} \\ \vdots & \vdots & \ddots & \vdots \\ A_{N1} & A_{N2} & \cdots & A_{NN} \end{bmatrix}, \\ B &= \mathrm{diag}[B_1 \quad B_2 \quad \cdots \quad B_N], \\ C &= \mathrm{diag}[C_1 \quad C_2 \quad \cdots \quad C_N], \\ F &= \mathrm{diag}[F_1 \quad F_2 \quad \cdots \quad F_N], \\ A_{ii} &= \begin{bmatrix} -\frac{D_i}{M_i} & \frac{1}{M_i} & 0 & 0 & -\frac{1}{M_i} \\ 0 & -\frac{1}{T_{ch,i}} & \frac{1}{T_{ch,i}} & 0 & 0 \\ -\frac{1}{R_i T_{g,i}} & 0 & -\frac{1}{T_{g,i}} & 0 & 0 \\ \beta_i & 0 & 0 & 0 & 1 \\ 2\pi \sum_{j=1, j\neq i}^{N} T_{ij} & 0 & 0 & 0 & 0 \end{bmatrix}, \\ A_{ij} &= \begin{bmatrix} 0 & 0 & 0 & 0 & 0 \\ 0 & 0 & 0 & 0 & 0 \\ 0 & 0 & 0 & 0 & 0 \\ 0 & 0 & 0 & 0 & 0 \\ -2\pi T_{ij} & 0 & 0 & 0 & 0 \end{bmatrix}, \qquad i \neq j, \\ B_i &= [0 \quad 0 \quad \tfrac{1}{T_{g,i}} \quad 0 \quad 0]^T, \\ C_i &= \begin{bmatrix} \beta_i & 0 & 0 & 0 & 1 \\ 0 & 0 & 0 & 1 & 0 \end{bmatrix}, \\ F_i &= [-\tfrac{1}{M_i} \quad 0 \quad 0 \quad 0 \quad 0]^T, \\ T_{ij} &= T_{ji}. \end{aligned}$$

In a multi-area LFC system, the control target of each area is to maintain the system frequency, as well as the scheduled tie-line power exchange. Hence, the ACE of each control area is generally defined as a linear combination of the frequency and the tie-line power exchange deviation:

$$ACE_i = \beta_i \Delta f_i + \Delta P_{tie,i}. \tag{2}$$

As shown in Fig. 1, the output of the PI controller is sampled and held by a clock-driven zero-order hold (ZOH) with a constant sampling interval, and all delays are aggregated into a single delay after the ZOH. As a result, the control command $u_i(t)$ received by the generation unit can be expressed as:

$$\begin{aligned} u_i(t) &= -K_{P,i} ACE_i - K_{I,i} \int ACE_i \\ &= -K_i y_i(s_k) = -K_i C_i x_i(s_k), \\ & \qquad s_k + \tau_i(s_k) \leq t < s_{k+1} + \tau_i(s_{k+1}), \end{aligned} \tag{3}$$

where $K_i = [K_{P,i} \quad K_{I,i}]$; $0 = s_0 < s_1 < \cdots < s_k < \cdots$ represent the sampling moments of the ZOH, with the interval between two successive sampling moments being time-invariant and defined as the LFC period $T = s_{k+1} - s_k$. The transmission delay $\tau_i(t)$ can be time-invariant or time-varying and satisfies:

$$\tau_i(t) \in [\underline{\tau} \quad \overline{\tau}], \quad -1 < \mu_1 \leq \dot{\tau}_i(t) \leq \mu_2 < 1, \tag{4}$$

where $0 \leq \underline{\tau} \leq \overline{\tau}$. Define $t_k = s_k + \tau_i(s_k)$ as the updating moment of $u_i(t)$. Note that the condition $\dot{\tau}_i(t) > -1$ guarantees that the sequence of t_k is strictly increasing, thereby ensuring causality. The interval between two successive updating moments of $u_i(t)$ is defined as:

$$\begin{aligned} \bar{T}_k &= t_{k+1} - t_k = s_{k+1} + \tau_i(s_{k+1}) - s_k - \tau_i(s_k) \\ &= T + \tau_i(s_{k+1}) - \tau_i(s_k). \end{aligned} \tag{5}$$

It is bounded by:

$$\mathcal{T}_1 = \max(T - \Delta\tau, 0) \leq \bar{T}_k \leq \mathcal{T}_2 = T + \Delta\tau, \tag{6}$$

where $\Delta\tau = \min(\overline{\tau} - \underline{\tau}, \max(|\mu_2 T|, |\mu_1 T|))$. When the transmission delay is time-invariant, the updating interval of $u_i(t)$ equals the LFC period, i.e., $\bar{T}_k = \mathcal{T}_1 = \mathcal{T}_2 = T$. In contrast, when the transmission delay is time-varying, the updating interval of $u_i(t)$ is not constant, which can affect generation operation.

There exist multiple transmission delays $\tau_i(t)$, $i = 1, 2, \cdots, N$ in a multi-area LFC system. In order to simplify the analysis and reduce the computational burden for multi-area LFC, it is assumed that the multiple transmission delays are all equal [10], [15], [16]. This single delay is denoted as $\tau(t)$. Substituting (3) into (1) gives the closed-loop system model of multi-area LFC:

$$\begin{aligned} \dot{x}(t) = Ax(t) + A_d x(t_k - \tau(s_k)) + F\Delta P_d, \\ t_k \leq t < t_{k+1}, \end{aligned} \tag{7}$$

where

$$A_d = \sum_{i=1}^{N} A_{d,i}, \quad A_{d,i} = \mathrm{diag}[0 \ \cdots \ -B_i K_i C_i \ \cdots \ 0].$$

Remark 1: As a well-known method for delay-dependent stability analysis, the input delay approach can be used for systems with both transmission delay and sampling [29]–[31]. When the input delay approach is used, an aggregate delay is usually considered, that is $\delta(t) = t - s_k$ when $t_k \leq t < t_{k+1}$. This $\delta(t)$ is bounded as:

$$\delta(t) \in [\underline{\tau} \quad \overline{\tau} + T], \quad \dot{\delta}(t) \leq 1, \qquad t_k \leq t < t_{k+1}. \tag{8}$$

An illustration of such delay is shown in Fig. 2. With condition (8) of the aggregate delay $\delta(t)$ taken into account, the LFC model can be rewritten:

$$\begin{aligned} \dot{x}(t) = Ax(t) + A_d x(t - \delta(t)) + F\Delta P_d, \\ t_k \leq t < t_{k+1}. \end{aligned} \tag{9}$$

Based on (9), the stability analysis methods proposed in [13]–[17], [26] for LFC systems with only time-varying delays

This article has been accepted for publication in a future issue of this journal, but has not been fully edited. Content may change prior to final publication. Citation information: DOI 10.1109/TPWRS.2020.2980883, IEEE Transactions on Power Systems

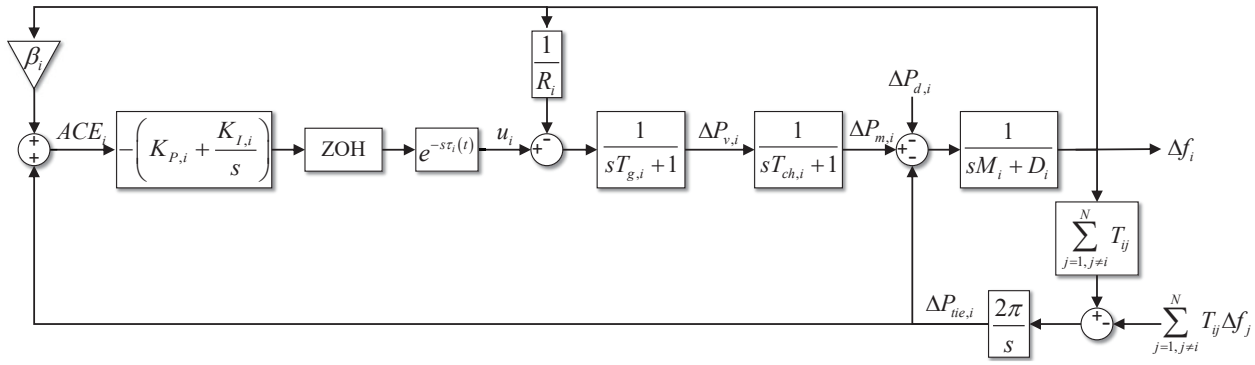

Fig. 1. Block diagram of the i-th control area in a multi-area LFC system.

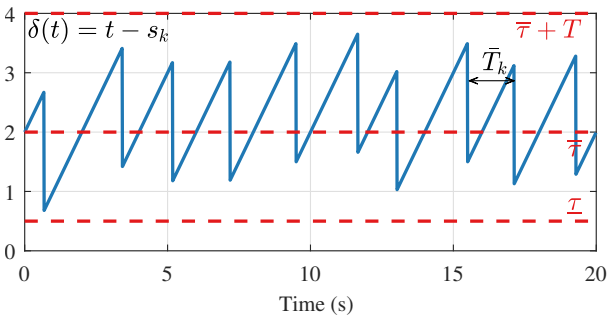

Fig. 2. An illustrative example of aggregate delay generated with an LFC period of $T = 2s$ and the transmission delay $\tau(t)$ bounded by $\underline{\tau} = 0.5s$ and $\bar{\tau} = 2s$.

can be extended to systems with both transmission delay and sampling. However, the aggregate delay with condition (8) fails to take into account the underlying characteristics of transmission and sampling-induced delays, where the latter is defined as $\kappa(t) = t - t_k$ when $t_k \leq t < t_{k+1}$. More specifically, no consideration is given to the rate limit of the transmission delay $\mu_1 \leq \dot{\tau}(t) \leq \mu_2$ nor the particular form of the sampling-induced delay, which results in $\dot{\kappa}(t) = 1$ when $t_k < t < t_{k+1}$. Therefore, it leads to relatively conservative results, with an illustration provided in Section V.

III. Delay-Dependent Stability Analysis

In delay-dependent stability analysis, the target is to find a transmission delay margin τ^* which ensures that the delay-dependent system is asymptotically stable for $\tau \leq \tau^*$, though it may become unstable for transmission delays that exceed the margin, $\tau > \tau^*$. In a delay-dependent system with both sampling and transmission delay, the delay margin results are helpful to evaluate system stability and determine an appropriate sampling interval.

To find the transmission delay margin, a new stability criterion for linear systems with both sampling and transmission delay is proposed. This new approach is based on a novel framework for stability analysis that utilizes the discrete-time Lyapunov Theorem with a continuous-time system model [25]. To reduce conservativeness of the stability criterion, the following techniques are involved:

1) The Wirtinger-based integral inequality and its affine version (see Lemma 2 of Appendix A) are both used and carefully chosen to derive a stability criterion. A convex condition is obtained directly without the use of reciprocally convex combinations.
2) A proper augmented Lyapunov-Krasovskii functional is chosen to fully benefit from the Wirtinger-based integral inequality. Common techniques for reducing conservativeness, through bounding the time derivative of the functional, have been applied [32].
3) Though the LFC system of interest is sampled periodically, the inclusion of time-varying delay means it shares some similarities with aperiodic sampled-data systems. Hence, a new technique developed for aperiodic sampled-data systems [33] is also introduced and modified to further reduce conservativeness.

A. Delay-Dependent Stability Criterion

This subsection presents a new stability criterion for systems with both sampling and transmission delay. Some helpful lemmas used in the proof of the proposed criterion are included in Appendix A.

Theorem 1: Consider the sampled-data system with transmission delay:

$$\dot{x}(t) = Ax(t) + A_d x(t_k - \tau(s_k)), \quad t_k \leq t < t_{k+1}, \tag{10}$$

where the time-varying delay satisfies (4), and hence the updating interval $\bar{T}_k = t_{k+1} - t_k$ satisfies (6). This system is asymptotically stable if there exist matrices $P \in \mathbb{S}_+^{4n}$; Q_1, Q_2, Q_3, $Q_{23} = Q_2 - Q_3$, S_1, S_2, $R \in \mathbb{S}_+^n$; L_1, $L_2 \in \mathbb{S}_+^{2n}$; $J \in \mathbb{S}^{4n}$; X_1, $X_2 \in \mathbb{R}^{3n\times 2n}$; U_1, $U_2 \in \mathbb{R}^{4n\times 4n}$; $H \in \mathbb{R}^{2n\times 2n}$; Y_1, $Y_2 \in \mathbb{R}^{12n\times 2n}$ that satisfy, for $i = 1, 2$, $j = 1, 2$, and $k = 1, 2$,

$$\begin{bmatrix} \Theta_1(h_j) + \mathcal{T}_i\Theta_{4-k} & \mathcal{T}_i Y_k & \hat{\tau} G_{3-j}^T X_{3-j} \\ \mathcal{T}_i Y_k^T & -\mathcal{T}_i L_k & 0_{2n\times 2n} \\ \hat{\tau} G_{3-j} X_{3-j}^T & 0_{2n\times 2n} & -\hat{\tau}\hat{S}_2 \end{bmatrix} \prec 0, \tag{11}$$

where

$$\Theta_1(\tau) = \mathrm{He}(M_1^T(\tau) P M_2) + e_1^T Q_1 e_1 - e_3^T (Q_1 - Q_2) e_3 - (1-\mu_2) e_2^T Q_{23} e_2 - e_4^T Q_3 e_4 - \frac{1}{1-\mu_1} e_5^T R e_5$$

$$
\begin{aligned}
&+ e_0^T(R + \underline{\tau}S_1 + \hat{\tau}S_2)e_0 - \frac{1}{\underline{\tau}}\Gamma_2^T\hat{S}_1\Gamma_2 \\
&- G_1^T\mathrm{He}(X_1\Gamma_1)G_1 - G_2^T\mathrm{He}(X_2\Gamma_1)G_2 \\
&+ \mathrm{He}(\Pi_1^T U_1\Pi_2 + \Pi_1^T U_2\Pi_8) - \mathrm{He}(Y_1N_{12} - Y_2N_{13}) \\
&+ \mathrm{He}(N_0^T H N_{13} + N_{12}^T H N_0), \\
\Theta_2 = &\ \mathrm{He}(\Pi_3^T U_1\Pi_4 + \Pi_5^T U_1\Pi_2 + \Pi_5^T U_2\Pi_8) + \Pi_8^T J\Pi_8 \\
&+ N_0^T L_1 N_0, \\
\Theta_3 = &\ \mathrm{He}(\Pi_6^T U_1\Pi_4 + \Pi_7^T U_1\Pi_2 + \Pi_7^T U_2\Pi_8) - \Pi_8^T J\Pi_8 \\
&+ N_0^T L_2 N_0,
\end{aligned}
$$

and

$$
\begin{aligned}
e_i &= [0_{n\times(i-1)n} \quad I_n \quad 0_{n\times(12-i)n}], \quad i = 1, 2, \cdots, 12, \\
e_0 &= Ae_1 + A_d e_7, \quad \hat{\tau} = \overline{\tau} - \underline{\tau}, \quad h_1 = \underline{\tau}, \quad h_2 = \overline{\tau}, \\
M_1(\tau) &= [e_1^T \quad e_2^T \quad \underline{\tau}e_{10}^T \quad (\tau - \underline{\tau})e_{11}^T + (\overline{\tau} - \tau)e_{12}^T]^T, \\
M_2 &= [e_0^T \quad e_5^T \quad e_1^T - e_3^T \quad e_3^T - e_4^T]^T, \\
\Gamma_1 &= \begin{bmatrix} I_n & -I_n & 0_{n\times n} \\ I_n & I_n & -2I_n \end{bmatrix}, \\
\Gamma_2 &= [e_1^T - e_3^T \quad e_1^T + e_3^T - 2e_{10}^T]^T, \\
G_1 &= [e_3^T \quad e_2^T \quad e_{11}^T]^T, \quad G_2 = [e_2^T \quad e_4^T \quad e_{12}^T]^T, \\
N_0 &= [e_0^T \quad e_5^T]^T, \quad N_1 = [e_1^T \quad e_2^T]^T, \quad N_2 = [e_6^T \quad e_7^T]^T, \\
N_3 &= [e_8^T \quad e_9^T]^T, \quad N_{12} = N_1 - N_2, \quad N_{13} = N_1 - N_3, \\
\Pi_1 &= [-N_{12}^T \quad N_{13}^T]^T, \quad \Pi_2 = [N_{12}^T \quad N_{13}^T]^T, \\
\Pi_3 &= [N_{12}^T \quad 0_{2n\times 12n}^T]^T, \quad \Pi_4 = [N_0^T \quad N_0^T]^T, \\
\Pi_5 &= [N_0^T \quad 0_{2n\times 12n}^T]^T, \quad \Pi_6 = [0_{2n\times 12n}^T \quad N_{13}^T]^T, \\
\Pi_7 &= [0_{2n\times 12n}^T \quad N_0^T]^T, \quad \Pi_8 = [N_2^T \quad N_3^T]^T, \\
\hat{S}_1 &= \mathrm{diag}(S_1, 3S_1), \quad \hat{S}_2 = \mathrm{diag}(S_2, 3S_2).
\end{aligned}
$$

Proof. Refer to Appendix B. □

Remark 2: One concern with this LMI-based criterion is its computational complexity for large-scale power systems. This disadvantage can be largely alleviated, however, by exploiting the structural features of LFC systems. For instance, the sparsity and symmetry of the system matrices in LFC systems can be exploited to significantly reduce the number of decision variables in LMIs [28], and the LFC model can be reconstructed into a delay-free part and a delay-related part to simplify the stability criterion with lower order [34]. Furthermore, parallel computing techniques can also be used to solve large-scale LMIs by exploiting sparsity to decompose them into smaller problems [35].

Remark 3: Although Theorem 1 is derived for time-varying transmission delay, it requires only minor changes to be used for stability analysis of systems with time-invariant transmission delay. In this latter case, the terms that include $\overline{\tau}$ are no longer required, so the corresponding matrices should be eliminated. Additionally, the rate limit on the transmission delay should have $\mu_1 = \mu_2 = 0$. The stability criterion for time-invariant transmission delay can be obtained following derivation similar to that of Theorem 1. It is omitted due to space limitation.

Remark 4: Theorem 1 can also be used for cases without sampling by setting the LFC period to a small value, e.g., $T = 10^{-3}s$.

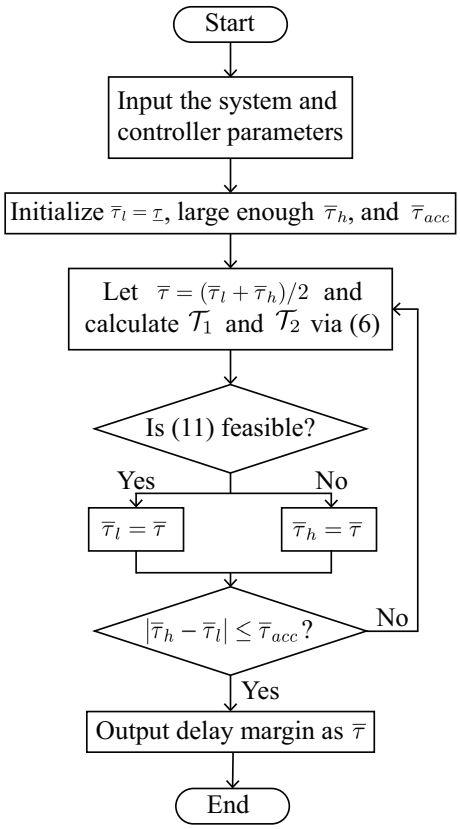

Fig. 3. Flow chart for determining the maximum allowable transmission delay for LFC systems.

B. Analysis Method

To find the delay margin, the conditions of Theorem 1 are integrated into the following constrained optimization problem [26]:

$$
\begin{aligned}
\textbf{P1:} \quad &\max \quad \overline{\tau} \\
&\text{s.t.} \quad (11), \qquad i = 1, 2, \quad j = 1, 2, \quad k = 1, 2.
\end{aligned}
$$

where $\underline{\tau}$, μ_1, μ_2 and T are given.

Problem **P1** is non-convex, so it cannot be solved directly. Nevertheless, for a given $\overline{\tau}$, the feasibility of the stability conditions (11) can be checked using off-the-shelf convex optimization software. Accordingly, a one-dimensional search method, i.e., binary search [13], and the commercial optimization solver MOSEK [36] have been used to determine the maximal allowable transmission delay for which (11) remains feasible. The steps for determining maximal allowable transmission delay are shown in Fig. 3.

IV. Case Studies

In this section, the transmission delay margins of a one-area and a two-area LFC system are calculated based on the method proposed in the previous section. For comparison purposes, the LFC system parameters given in [13] and provided in Table I are used, and the PI gains of the LFC controllers in each control area are assumed to be equal. The default LFC period is chosen as $T = 2s$. To show the advantage of the proposed method, the stability analysis methods proposed in [13] and

This article has been accepted for publication in a future issue of this journal, but has not been fully edited. Content may change prior to final publication. Citation information: DOI 10.1109/TPWRS.2020.2980883, IEEE Transactions on Power Systems

TABLE I
PARAMETERS OF LFC SYSTEMS (IN P.U.)

Parameter	M	D	β	T_g	T_{ch}	R	T_{12}
Area 1	10	1.0	21.0	0.1	0.3	0.05	0.1986
Area 2	12	1.5	21.5	0.17	0.4	0.05	

[26] are used with the condition (8) in Remark 1 as benchmarks. Time-domain simulation of the LFC systems is also undertaken in MATLAB/Simulink to verify the transmission delay margin results calculated by the proposed method.

A. Time-Invariant Transmission Delay

Considering a one-area LFC system with time-invariant transmission delay and sampling, the delay margins are calculated using Theorem 1 for various PI controller gains and are compared with the results obtained by [13], [26]. This comparison is provided in Table II. Note that the stability analysis methods presented in [13], [26] can only provide delay margins for the time-varying aggregate delay $\delta(t)$, so the results in Table II are obtained by subtracting the LFC period T from the initial results to give the margins for the transmission delay. The symbol '-' denotes cases where asymptotic stability cannot be guaranteed by the methods.

Table II clearly shows that Theorem 1 provides larger transmission delay margins than the methods proposed in [13], [26], especially for the cases where $K_P > 0$. Additionally, the methods proposed in [13], [26] fail to ensure asymptomatic stability of the LFC system in many cases where Theorem 1 does give such a guarantee. This is because aggregating the transmission and sampling-induced delays into an aggregate delay by condition (8) neglects their different characteristics, leading to more conservative results.

The results obtained by Theorem 1 also show that for a given K_P the transmission delay margin decreases rapidly as K_I increases, which indicates that the LFC system is less stable for higher K_I. For a given K_I, it can be seen that the transmission delay margin initially increases then decreases with increasing K_P. Observations in [10], [13] indicate a similar impact of K_P and K_I on delay margins. This pattern can be used to guide the tuning of the LFC controller to allow maximal transmission delay margin or a trade-off between dynamic performance and transmission delay margin [18], [37].

Time-domain simulations of the studied system were also undertaken to verify the delay margin results obtained by Theorem 1. The frequency response of the one-area LFC system with PI controller $K_p = 0.1$, $K_I = 0.15$, and LFC period $T = 2s$ under different constant transmission delays are shown in Fig. 4. A positive load disturbance $\Delta P_d = 0.1$ is added to the system at $t = 10s$. Simulation results indicate that the transmission delay margin lies in the interval $[9.37, 9.54]$ seconds, which demonstrates that the one-area LFC system is asymptotically stable at the obtained value of $9.37s$ shown in Table II. Furthermore, this value is close to the actual delay margin. For $K_p = 0$, $K_I = 0.4$, the delay margin obtained by the proposed method is $2.18s$, while the method in [13] cannot find a stable region and the method in [26]

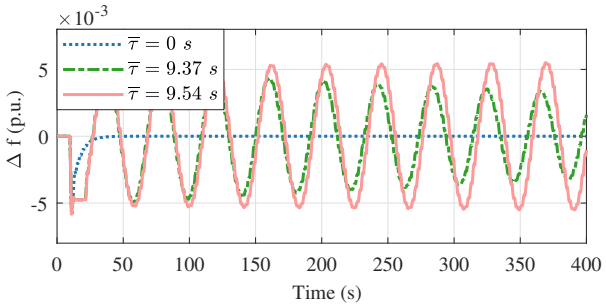

Fig. 4. Frequency deviation of the one-area LFC system ($K_p = 0.1$, $K_I = 0.15$) under different time-invariant transmission delays.

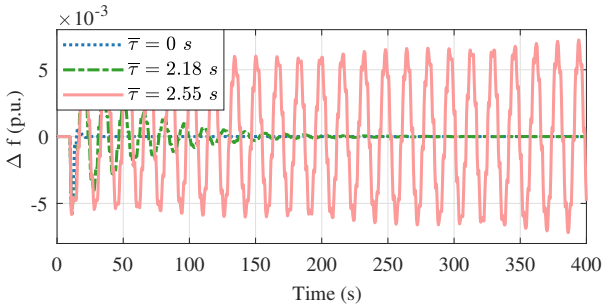

Fig. 5. Frequency deviation of the one-area LFC system ($K_p = 0$, $K_I = 0.4$) under different time-invariant transmission delays.

gives the delay margin as $0.85s$. The simulations presented in Fig. 5 show that the actual delay margin lies in the interval $[2.18, 2.55]$ seconds, which again shows the effectiveness and advantage of the proposed method.

B. Time-Varying Transmission Delay

A two-area LFC system with time-varying transmission delay and sampling is now studied. For the use of Theorem 1, consider $\underline{\tau} = 10^{-4}$, and the two cases $-\mu_1 = \mu_2 = 0.2$ and 0.5, respectively denoted by the superscripts ^{1} and ^{2} in Table III. The transmission delay margin results are summarized in Table III, where the effects of the PI controller gains on transmission delay margins are similar to those of the earlier case. It can be observed that the delay margins obtained by Theorem 1 improve on the results of [13], [26], especially for cases with larger K_P. Note that the constraints on the rate limit of the transmission delays are taken into account in the conditions of Theorem 1. However, the methods proposed in [13], [26] with condition (8) cannot utilize such information, leading to more conservative results.

Time-domain simulations with time-varying delays are then undertaken. Similar to the simulations in Section IV-A, a positive load disturbance $\Delta P_d = 0.1$ is added in area 1 at $t = 10s$. The time-varying delay is implemented using a sine wave with a bias. For $K_p = 0.1$, $K_I = 0.15$, the results in Table III show that the two-area LFC system is stable with time-varying delay smaller than $6.81s$ with a rate limit $-\mu_1 = \mu_2 = 0.5$. To verify this result, the time-varying delay $\tau(t) = 6.31 + 0.5\sin(t)$ is implemented. The frequency response of the corresponding two-area LFC system is shown in Fig. 6, which demonstrates the asymptotic stability of the

This article has been accepted for publication in a future issue of this journal, but has not been fully edited. Content may change prior to final publication. Citation information: DOI 10.1109/TPWRS.2020.2980883, IEEE Transactions on Power Systems

TABLE II
TRANSMISSION DELAY MARGINS OBTAINED BY THEOREM 1, [13], AND [26] FOR THE TIME-INVARIANT CASE (ONE-AREA LFC)

$\overline{\tau}$	K_P														
	0			0.05			0.1			0.2			0.4		
K_I	Th. 1	[13]	[26]	Th. 1	[13]	[26]	Th. 1	[13]	[26]	Th. 1	[13]	[26]	Th. 1	[13]	[26]
0.05	29.79	15.31	24.38	30.67	5.47	12.23	31.32	1.91	5.51	31.87	-	1.61	26.95	-	-
0.1	14.08	6.41	10.97	14.54	4.05	8.91	14.88	1.64	4.88	15.30	-	1.51	14.00	-	-
0.15	8.83	3.44	6.50	9.13	2.70	6.12	**9.37**	1.28	4.07	9.63	-	1.36	8.97	-	-
0.2	6.19	1.96	4.25	6.42	1.69	4.22	6.59	0.90	3.23	6.77	-	1.18	6.32	-	-
0.4	**2.18**	-	0.85	2.29	-	0.92	2.37	-	0.87	2.45	-	0.36	2.07	-	-
0.6	0.83	-	-	0.90	-	-	0.95	-	-	1.01	-	-	0.85	-	-
1	0.07	-	-	0.11	-	-	0.15	-	-	0.20	-	-	-	-	-

TABLE III
TRANSMISSION DELAY MARGINS OBTAINED BY THEOREM 1, [13], AND [26] FOR THE TIME-VARYING CASE (TWO-AREA LFC)

$\overline{\tau}$	K_P															
	0				0.05				0.1				0.2			
K_I	Th. 1^1	Th. 1^2	[13]	[26]	Th. 1^1	Th. 1^2	[13]	[26]	Th. 1^1	Th. 1^2	[13]	[26]	Th. 1^1	Th. 1^2	[13]	[26]
0.05	26.72	25.07	13.26	23.57	27.32	25.78	5.11	11.87	27.47	26.02	1.81	5.31	26.41	23.50	-	1.51
0.1	12.45	11.10	5.83	10.46	12.82	11.51	3.71	8.44	13.03	11.70	1.54	4.69	12.85	11.01	-	1.40
0.15	7.58	6.38	2.20	6.08	7.86	6.65	1.74	5.53	8.03	**6.81**	1.16	3.87	7.98	6.48	-	1.26
0.2	**5.10**	3.99	0.09	3.87	5.31	4.19	-	3.69	5.46	4.31	-	2.89	5.47	4.12	-	1.09
0.4	1.27	0.65	-	0.50	1.37	0.69	-	0.53	1.45	0.72	-	0.46	1.48	0.69	-	0.06
0.6	0.22	0.17	-	-	0.25	0.19	-	-	0.27	0.21	-	-	0.28	0.22	-	-
1	-	-	-	-	-	-	-	-	-	-	-	-	-	-	-	-

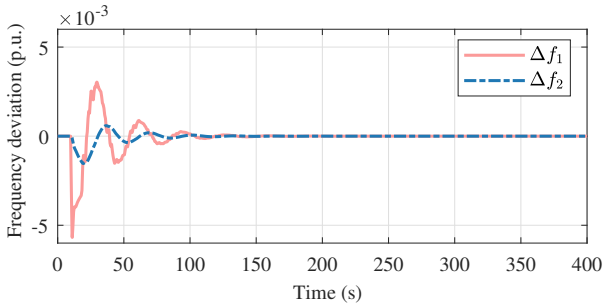

Fig. 6. Frequency deviation of the two-area LFC system ($K_p = 0.1$, $K_I = 0.15$) under time-varying transmission delay $\tau(t) = 6.31 + 0.5\sin(t)$.

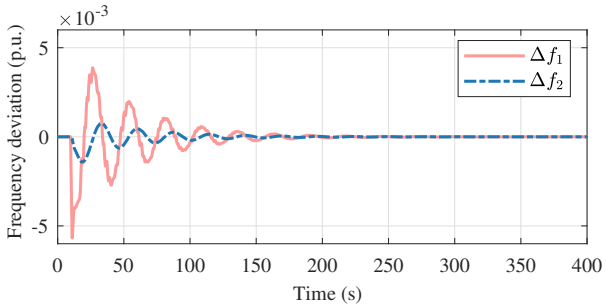

Fig. 7. Frequency deviation of the two-area LFC system ($K_p = 0$, $K_I = 0.2$) under time-varying transmission delay $\tau(t) = 4.90 + 0.2\sin(t)$.

studied system. Fig. 7 shows the frequency response with $K_p = 0$, $K_I = 0.2$ under time-varying transmission delay $\tau(t) = 4.90 + 0.2\sin(t)$, which also verifies the delay margin $5.10s$ given in Table III.

C. Discussion

1) Effect of Sampling Interval: The one-area LFC system with time-invariant transmission delay is used to explore the effect of sampling interval on transmission delay margin. Table IV lists the transmission delay margin results obtained by Theorem 1 with different sampling intervals. It is worth noting that the delay margin results with $T = 10^{-3}s$ shown in Table IV improve on those in [13], [26], where sampling is not considered. This indicates that Theorem 1 is also effective for delay-dependent stability analysis without sampling.

Table IV clearly shows that the transmission delay margin decreases as the sampling interval increases. In most cases the declining rate of the delay margin is less than the ascending rate of the sampling interval, the exception being some cases when $K_p = 0.4$. This characteristic suggests that Theorem 1 outperforms other methods by separately considering transmission and sampling-induced delays.

2) Effect of ACE Filtering: In practical LFC systems, ACE signals are generally filtered to smooth out noise and avoid unnecessary control actions, before being used as the inputs of PI controllers. To this end, low-pass filters (LPFs) can be applied [8]. To show the effect of ACE filtering on delay margins, a first-order LPF is added just before the PI controller of each area, and the state-space model of the multi-area LFC system (1) is trivially modified to include the LPFs.

The delay margins obtained by Theorem 1 for one-area and two-area LFC systems with the first-order LPFs are shown in Figs. 8 and 9. Both figures show that the inclusion of LPFs reduces the delay margins, and the delay margins decrease as the time constants of the LPFs increase. These observations can be explained by the fact that first-order LPFs not only filter noise but also introduce phase delays and thus reduce transmission delay margins. In addition, the larger the time constant of the first-order LPFs, the larger the phase delay,

This article has been accepted for publication in a future issue of this journal, but has not been fully edited. Content may change prior to final publication. Citation information: DOI 10.1109/TPWRS.2020.2980883, IEEE Transactions on Power Systems

TABLE IV
TRANSMISSION DELAY MARGINS OBTAINED BY THEOREM 1 WITH DIFFERENT SAMPLING INTERVALS (ONE-AREA LFC)

$\overline{\tau}$	K_P														
	0			0.05			0.1			0.2			0.4		
K_I \ T	10^{-3}	1	2	10^{-3}	1	2	10^{-3}	1	2	10^{-3}	1	2	10^{-3}	1	2
0.05	30.85	30.33	29.79	31.80	31.26	30.67	32.66	32.06	31.32	32.76	32.76	31.87	28.42	28.42	26.95
0.1	15.17	14.65	14.08	15.65	15.12	14.54	16.08	15.53	14.88	16.8	16.15	15.30	16.76	16.27	14.00
0.15	9.94	9.41	8.83	10.26	9.73	9.13	10.55	10.01	9.37	11.03	10.45	9.63	11.21	10.69	8.97
0.2	7.32	6.79	6.19	7.56	7.02	6.42	7.78	7.23	6.59	8.14	7.57	6.77	8.37	7.79	6.32
0.4	3.38	2.83	2.18	3.50	2.95	2.29	3.60	3.05	2.37	3.78	3.21	2.45	3.97	3.32	2.07
0.6	2.04	1.48	0.83	2.12	1.56	0.90	2.19	1.63	0.95	2.31	1.73	1.01	2.42	1.78	0.85
1	0.92	0.37	0.07	0.97	0.41	0.11	1.01	0.45	0.15	1.08	0.50	0.20	1.12	0.50	-

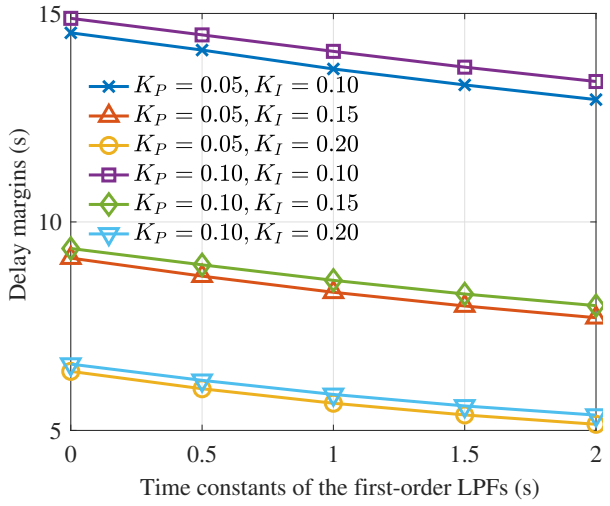

Fig. 8. Delay margins obtained by Theorem 1 for one-area LFC systems with first-order LPFs and constant delays.

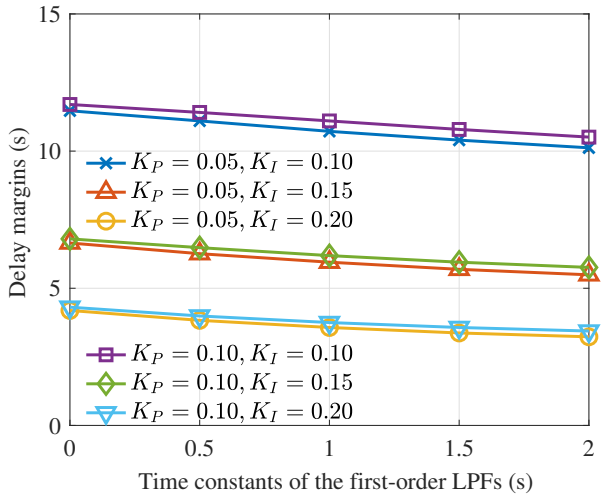

Fig. 9. Delay margins obtained by Theorem 1 for two-area LFC systems with first-order LPFs and time-varying delays ($-\mu_1 = \mu_2 = 0.5$).

leading to smaller transmission delay margins.

3) Incorporating BSSs: BSSs with fast response speeds and rapid ramping capabilities are competitive for LFC and have drawn much attention. To manage a large-scale BSS consisting of many battery storage packs or distributed BSSs in LFC, multi-layer communication networks are generally used, where the delays cannot be ignored [6]. To investigate the impacts of incorporating BSSs on LFC, the i-th control area model in Fig. 1 is modified to include a BSS model, as shown in Fig 10. The power commands for the non-reheat generation unit and the BSS are determined depending on their participation factors $\alpha_{G,i}$ and $\alpha_{B,i}$.

Figs. 11 and 12 show the delay margins obtained by Theorem 1 for one-area and two-area LFC systems with BSSs. It can be observed that an increase of α_B would slightly increase the resulting delay margins. These results indicate that incorporating BSSs helps stabilize the delayed LFC, though trivially. It is worth noting that our observations are consistent with the conclusions of [38] but inconsistent with the conclusions of [17], which shows that incorporating BSSs would decrease the delay margins. A reason for the different observations may be the different generator types (non-reheat generation unit in [38] and our study, while reheat generation unit in [17]). Hence, it can be inferred that the impacts of BSSs on the delay margins of LFC systems are dependent on other system conditions.

D. Guidelines for LFC Design Considering Delay Margins

The delay margins obtained by the proposed criterion can be used to guide the design of LFC, e.g., tuning PI gains, choosing communication networks and sampling intervals.

1) In general, the PI gains of LFC controllers are chosen to achieve better transient performance. However, the results in Sections IV.A and IV.B indicate that larger PI gains may result in smaller delay margins and lead to LFC controllers that are less robust to delays. One way to consider delay-dependent stability at the design stage of LFC controllers is to choose the delay margin as an additional performance index and tune the PI gains to trade off between transient performance and delay margin.
2) The obtained results also show that the delay margin decreases as the rate limit of the time-varying delay increases. This suggests that communication networks where delays change more slowly are preferred in LFC.
3) Table IV indicates a non-linear relationship between LFC delay margin and sampling interval, one of the most interesting outcomes of this study. The results in Table IV show that a larger sampling interval generally results in a smaller delay margin. Thus, enlarging the

This article has been accepted for publication in a future issue of this journal, but has not been fully edited. Content may change prior to final publication. Citation information: DOI 10.1109/TPWRS.2020.2980883, IEEE Transactions on Power Systems

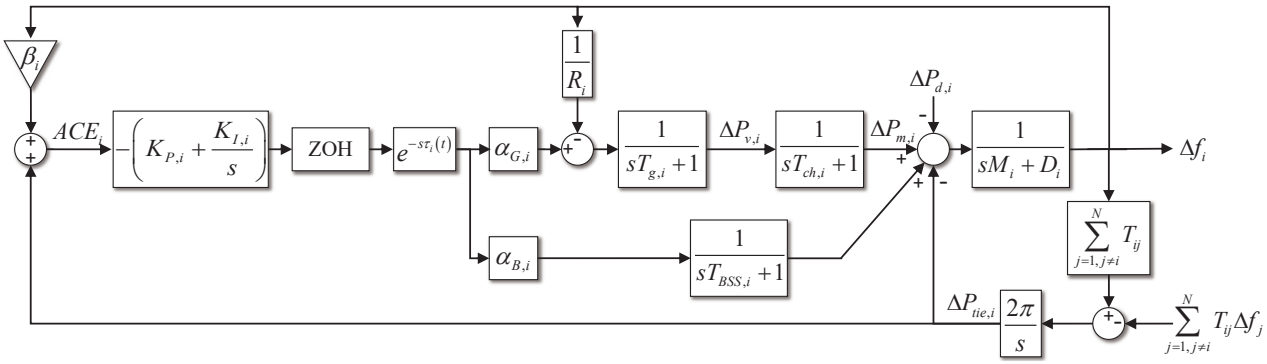

Fig. 10. Block diagram of the i-th control area in a multi-area LFC system with a BSS model included.

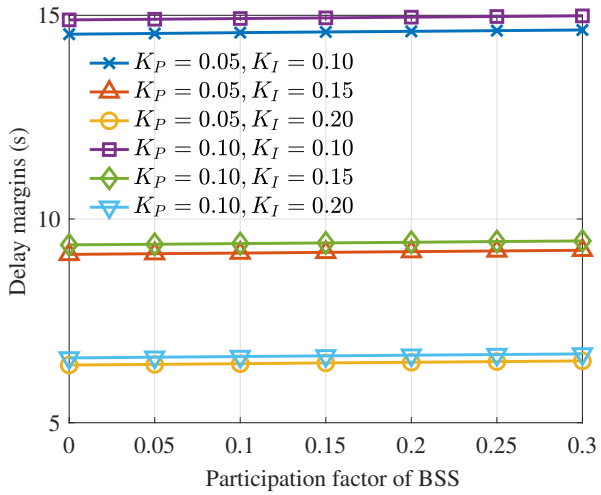

Fig. 11. Delay margins obtained by Theorem 1 for one-area LFC systems with a BSS ($T_{BSS} = 0.035s$) and constant delays.

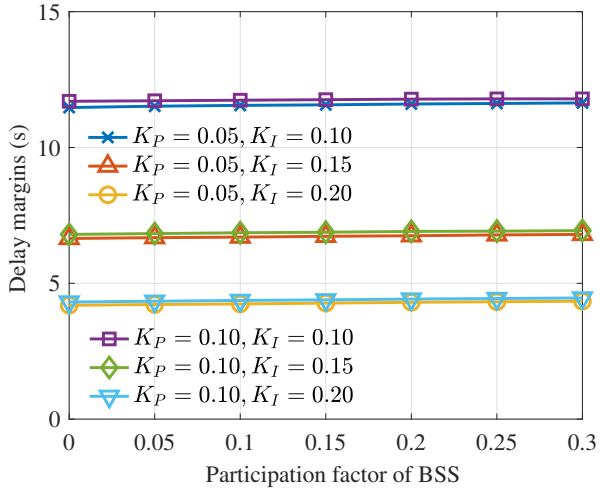

Fig. 12. Delay margins obtained by Theorem 1 for two-area LFC systems with BSSs ($T_{BSS} = 0.035s$) and time-varying delays ($-\mu_1 = \mu_2 = 0.5$).

sampling interval in LFC systems can decrease the communication rate but require a communication network with shorter delays. Effective LFC communication network designs must take this non-linear trade-off into account.

V. Conclusions

The stability of LFC systems with both sampling and transmission delay has been investigated. The conventional LFC model is modified to separately consider transmission delay and sampling. Based on Lyapunov stability theory and LMIs, a new stability criterion for linear systems with both sampling and transmission delay is proposed. The stability of one-area and two-area LFC systems with time-invariant and time-varying transmission delays has been analyzed for various values of the PI gains. Based on the results obtained in case studies, the findings are summerized as follows:

1) Compared with prior work, the proposed method can obtain larger stability regions for LFC systems. This follows from the separate consideration of transmission delay and sampling, as well as the choice of Lyapunov functionals and bounding techniques.
2) Time-domain simulations illustrate that delay margins obtained by the proposed method are close to the actual margins, highlighting the effectiveness of the proposed approach.
3) The impact of K_P and K_I values on delay margins is largely independent of whether sampling is considered or not.
4) Delay margins of LFC systems decrease as the sampling intervals increase, but the declining rates of delay margins are generally smaller than the ascending rate of the sampling interval. This characteristic has not been shown in previous delay-dependent stability studies for LFC systems.
5) The inclusion of an ACE filtering scheme may reduce the transmission delay margin since it introduce extra phase delays.

Transmission delays associated with different regulating units generically differ. Therefore LFC systems must maintain stability in the presence of multiple independent transmission delays. Our on-going work is addressing this important,

though nontrivial, question of LFC system stability with both sampling and multiple transmission delays. Generation rate limits (GRC) also affect stability of LFC systems. Future work will consider approaches to modeling GRC in delay-dependent stability analysis and ways of managing the nonlinearity that GRC introduces.

APPENDIX A
USEFUL LEMMAS

As in [24], define the function $\chi_k : [0, \bar{T}_k] \times [-\tau(s_k), 0] \to \mathbb{R}^n$, such that for all η in $[0, \bar{T}_k]$ and all θ in $[-\tau(s_k), 0]$, $\chi_k(\eta, \theta) = x(t_k + \eta + \theta)$. Let $\mathbb{K}$ denote the set of functions defined by χ_k, which is the set of continuous functions from $[0, \bar{T}_k] \times [-\overline{\tau}, 0]$ to $\mathbb{R}^n$.

Lemma 1 [24]: Let $V : \mathbb{K} \to \mathbb{R}^+$ be a differentiable functional for which there exist positive numbers $\sigma_1 < \sigma_2$ and p, such that for all $\chi_k \in \mathbb{K}$,

$$\sigma_1 |\chi_k(0,\cdot)|^p \le V(\chi_k(0,\cdot)) \le \sigma_2 |\chi_k(0,\cdot)|^p. \tag{12}$$

The following two statements are equivalent.

1) For all $k \in \mathbb{N}$ and all $\bar{T}_k \in [\mathcal{T}_1, \mathcal{T}_2]$,
$$\Delta V(k) = V(\chi_k(\bar{T}_k,\cdot)) - V(\chi_k(0,\cdot)) < 0; \tag{13}$$
2) There exists a continuous and differentiable functional $\mathcal{V} : \mathbb{R} \times \mathbb{K} \to \mathbb{R}$, which satisfies for all $k \in \mathbb{N}$ and all $\bar{T}_k \in [\mathcal{T}_1, \mathcal{T}_2]$,
$$\mathcal{V}(\bar{T}_k, \chi_k(\cdot,\cdot)) = \mathcal{V}(0, \chi_k(\cdot,\cdot)), \tag{14}$$
and for all $k \in \mathbb{N}$, all $\bar{T}_k \in [\mathcal{T}_1, \mathcal{T}_2]$, and all $\eta \in [0, \bar{T}_k]$,
$$\dot{\mathcal{W}}(\eta, \chi_k) = \frac{d}{d\eta}[V(\chi_k(\eta,\cdot)) - \mathcal{V}(\eta, \chi_k(\cdot,\cdot))] < 0. \tag{15}$$

In addition, if either of the two statements is satisfied, the system given in (7) is asymptotically stable.

Lemma 2 [39]: Let $x : [\alpha, \beta] \to \mathbb{R}^n$ be a differentiable function. Define $\varpi = [x^T(\beta) \quad x^T(\alpha) \quad \frac{1}{\beta-\alpha}\int_\alpha^\beta x^T(s)ds]^T$, and $\tilde{M} = \begin{bmatrix} I_n & -I_n & 0_{n\times n} \\ I_n & I_n & -2I_n \end{bmatrix}$. For any symmetric matrix $\tilde{R} \succ 0$ and $\bar{R} = \mathrm{diag}(\tilde{R}, 3\tilde{R})$, the following statements are true and equivalent:

1. The following inequality holds:
$$-\int_\alpha^\beta \dot{x}^T(s)\tilde{R}\dot{x}(s)ds \le -\varpi^T \tilde{\Omega}_1 \varpi \tag{16}$$
where $\tilde{\Omega}_1 = \frac{1}{\beta-\alpha}\tilde{M}^T\bar{R}\tilde{M}$.

2. There exists a matrix $\tilde{X} \in \mathbb{R}^{3n\times 2n}$ such that the following inequality holds:
$$-\int_\alpha^\beta \dot{x}^T(s)\tilde{R}\dot{x}(s)ds \le -\varpi^T \tilde{\Omega}_2 \varpi \tag{17}$$
where $\tilde{\Omega}_2 = \mathrm{He}(\tilde{X}\tilde{M}) - (\beta-\alpha)\tilde{X}\bar{R}^{-1}\tilde{X}^T$.

Lemma 3: For $U \in \mathbb{S}_+^n$, $Y \in \mathbb{R}^{m\times n}$, $w \in \mathbb{R}^n$, and $v \in \mathbb{R}^m$, the following inequality always holds:
$$w^T U w \ge 2v^T Y w - v^T Y U^{-1} Y^T v. \tag{18}$$

Proof. The proof of Lemma 3 follows directly from the Schur complement condition [40]. □

APPENDIX B
PROOF OF THEOREM 1

Let $\gamma_k(\eta)$ and $\dot{\gamma}_k(\eta)$ represent the transmission delay $\tau(t) = \tau(t_k+\eta)$ and its derivative $\dot{\tau}(t) = \dot{\tau}(t_k+\eta)$, respectively. The following nomenclature is used:

$$\begin{aligned}
z(\eta) &= [\chi_k^T(\eta,0) \quad \chi_k^T(\eta,-\gamma_k(\eta))]^T,\\
\phi_1(\eta) &= [z^T(\eta) \quad \int_{-\underline{\tau}}^0 \chi_k^T(\eta,s)ds \quad \int_{-\overline{\tau}}^{-\underline{\tau}} \chi_k^T(\eta,s)ds]^T,\\
\phi_2(\eta) &= [(\bar{T}_k-\eta)(z^T(\eta)-z^T(0)) \quad \eta(z^T(\eta)-z^T(\bar{T}_k))]^T,\\
\phi_3(\eta) &= [(z^T(\eta)-z^T(0)) \quad (z^T(\eta)-z^T(\bar{T}_k))]^T,\\
\phi_4(\eta) &= [z^T(0) \quad z^T(\bar{T}_k)]^T,\\
\xi(\eta) &= [z^T(\eta) \quad \chi_k^T(\eta,-\underline{\tau}) \quad \chi_k^T(\eta,-\overline{\tau})\\
&\quad (1-\dot{\gamma}_k)\dot{\chi}_k^T(\eta,-\gamma_k(\eta)) \quad z^T(0) \quad z^T(\bar{T}_k)\\
&\quad \tfrac{1}{\underline{\tau}}\int_{-\underline{\tau}}^0 \chi_k^T(\eta,s)ds \quad \tfrac{1}{\gamma_k(\eta)-\underline{\tau}}\int_{-\gamma_k(\eta)}^{-\underline{\tau}} \chi_k^T(\eta,s)ds\\
&\quad \tfrac{1}{\overline{\tau}-\gamma_k(\eta)}\int_{-\overline{\tau}}^{-\gamma_k(\eta)} \chi_k^T(\eta,s)ds]^T.
\end{aligned}$$

Consider the following Lyapunov-Krasovskii functional candidate:

$$\begin{aligned}
V(\chi_k) = \phi_1^T(\eta)P\phi_1(\eta) &+ \int_{-\underline{\tau}}^0 \chi_k^T(\eta,s)Q_1\chi_k(\eta,s)ds\\
&+ \int_{-\gamma_k(\eta)}^{-\underline{\tau}} \chi_k^T(\eta,s)Q_2\chi_k(\eta,s)ds\\
&+ \int_{-\overline{\tau}}^{-\gamma_k(\eta)} \chi_k^T(\eta,s)Q_3\chi_k(\eta,s)ds\\
&+ \int_{-\gamma_k(\eta)}^0 \dot{\chi}_k(\eta,s)^T R\dot{\chi}_k(\eta,s)ds\\
&+ \int_{-\underline{\tau}}^0\int_\lambda^0 \dot{\chi}_k^T(\eta,s)S_1\dot{\chi}_k(\eta,s)dsd\lambda\\
&+ \int_{-\overline{\tau}}^{-\underline{\tau}}\int_\lambda^0 \dot{\chi}_k^T(\eta,s)S_2\dot{\chi}_k(\eta,s)dsd\lambda.
\end{aligned} \tag{19}$$

The looped-functional that utilizes the information on the interval $x(t_k)$ to $x(t)$ and $x(t)$ to $x(t_{k+1})$ is first introduced in [33] and is modified in this paper:

$$\begin{aligned}
\mathcal{V}(\eta,\chi_k) = &\,\mathrm{He}(\phi_2^T(\eta)(U_1\phi_3(\eta)+U_2\phi_4(\eta)))\\
&+ \mathrm{He}((z^T(\eta)-z^T(0))H(z(\eta)-z(\bar{T}_k)))\\
&+ (\bar{T}_k-\eta)\eta\phi_4^T(\eta)J\phi_4(\eta)\\
&+ (\bar{T}_k-\eta)\int_0^\eta \dot{z}^T(s)L_1\dot{z}(s)ds\\
&- \eta\int_\eta^{\bar{T}_k} \dot{z}^T(s)L_2\dot{z}(s)ds.
\end{aligned} \tag{20}$$

Remark 5: As we are studying the stability of LFC systems with both sampling and delay, $\mathcal{W} = V + \mathcal{V}$ proposed in this paper is related to both sampling and delay effects. If we neglect sampling effects and set $T = 0$, condition (14) and $\mathcal{V}$ will vanish and thus $\mathcal{W} = V$. In this case, the proposed functional will become a pure Lyapunov-Krasovskii functional for delayed systems, and includes the functionals in [13], [14], [26] as special cases. If we neglect delay effects, set $\tau(t) = 0$, and eliminate the delay-related terms, V will degenerate to a simple quadratic Lyapunov function and $\mathcal{V}$ will become a

looped-funtional for sampled-data systems. In this case, we will find that the proposed functional is more general when compared with the functionals for sampled-data systems in [25], [29]–[31], [33] and includes them as special cases. It is worth noting that the proposed functional also includes the functionals for networked control systems with both sampling and delay in [21], [24] as special cases, and the differences in augmented terms and looped functionals help to obtain a less conservative criterion.

The functional $\mathcal{V}$ satisfies the condition (14) because $\mathcal{V}(0,\chi_k) = \mathcal{V}(\bar{T}_k,\chi_k) = 0$. Since the objective here is to guarantee that the variation of $V(\chi_k)$ between two successive sampling moments is strictly negative by Lemma 1, the remainder of the proof ensures that $\dot{\mathcal{W}} < 0$ over the interval $[0,\bar{T}_k]$. The computation of $\dot{\mathcal{W}}$ results in (21).

For the terms in (21) that include $\dot{\gamma}_k(\eta)$, the positive definiteness of R and Q_{23} and the inequality $\mu_1 \le \dot{\tau}(t) = \dot{\gamma}_k(\eta) \le \mu_2$ are used to bound them.

The first integral term of (21) can be bounded by applying the first statement of Lemma 2:

$$-\int_{-\underline{\tau}}^{0} \dot{\chi}_k^T(\eta,s) S_1 \dot{\chi}_k(\eta,s) ds \le -\xi^T(\eta)(\frac{1}{\underline{\tau}} \Gamma_2^T \hat{S}_1 \Gamma_2)\xi(\eta). \tag{22}$$

The second integral term of (21) can be bounded using the second statement of Lemma 2:

$$\begin{aligned}
&-\int_{-\overline{\tau}}^{-\underline{\tau}} \dot{\chi}_k^T(\eta,s) S_2 \dot{\chi}_k(\eta,s) ds \\
&= -\int_{-\gamma_k(\eta)}^{-\underline{\tau}} \dot{\chi}_k^T(\eta,s) S_2 \dot{\chi}_k(\eta,s) ds - \int_{-\overline{\tau}}^{-\gamma_k(\eta)} \dot{\chi}_k^T(\eta,s) S_2 \dot{\chi}_k(\eta,s) ds \\
&\le -\xi^T(\eta)(G_1^T \mathrm{He}(X_1\Gamma_1)G_1 + G_2^T \mathrm{He}(X_2\Gamma_1)G_2 \\
&\quad - (\gamma_k(\eta)-\underline{\tau})X_1\hat{S}_2^{-1}X_1^T - (\overline{\tau}-\gamma_k(\eta))X_2\hat{S}_2^{-1}X_2^T)\xi(\eta).
\end{aligned} \tag{23}$$

Using Lemma 3, the third and fourth integral terms of (21) can be bounded:

$$\begin{aligned}
-\int_0^{\eta} \dot{z}^T(s) L_1 \dot{z}(s) ds - \int_{\eta}^{\bar{T}_k} \dot{z}^T(s) L_2 \dot{z}(s) ds \\
\le \xi^T(\eta)(\eta Y_1 L_1^{-1} Y_1^T + (\bar{T}_k - \eta) Y_2 L_2^{-1} Y_2^T \\
- \mathrm{He}(Y_1 N_{12} - Y_2 N_{13}))\xi(\eta).
\end{aligned} \tag{24}$$

As a result, the following inequality can be obtained:

$$\begin{aligned}
\dot{\mathcal{W}}(\eta,\chi_k) \le \xi^T(\eta)[&\Theta_1(\gamma_k(\eta)) + (\bar{T}_k - \eta)\Theta_2 + \eta\Theta_3 \\
&+ (\gamma_k(\eta)-\underline{\tau})X_1\hat{S}_2^{-1}X_1^T + (\overline{\tau}-\gamma_k(\eta))X_2\hat{S}_2^{-1}X_2^T \\
&+ \eta Y_1 L_1^{-1} Y_1^T + (\bar{T}_k - \eta) Y_2 L_2^{-1} Y_2^T]\xi(\eta).
\end{aligned} \tag{25}$$

Considering that the inner matrix at the right side of (25) is linear, and therefore convex, with respect to $\eta \in [0,\bar{T}_k]$, $\gamma_k(\eta) \in [\underline{\tau},\overline{\tau}]$, and $\bar{T}_k \in [\mathcal{T}_1,\mathcal{T}_2]$, the right side of (25) is negative definite if condition (11) is satisfied, by virtue of the Schur complement condition. Lemma 1 therefore ensures asymptotic stability of the system (7).

Remark 6: Although the two statements in Lemma 2 are equivalent, they are both used in the proof of Theorem 1. Note that the convexity of (25) in η, $\gamma_k(\eta)$, and $\bar{T}_k$ is important to obtain a tractable stability criterion. Since the first statement in Lemma 2 has less decision variables and its right term is linearly dependent on $\bar{R}$, it is usually more attractive. However, the first statement depends on the reciprocal of the length of the integral interval, $\beta - \alpha$, so when $\beta - \alpha$ is linear in η, $\gamma_k(\eta)$ or $\bar{T}_k$, convexity (in those variables) is lost. Though a convex approach can be used to retain the convexity, it would lead to more conservative results [41]. In this case, the second statement is more attractive due to its linear dependence on $\beta - \alpha$.

REFERENCES

[1] V. Donde, M. Pai, and I. A. Hiskens, "Simulation and optimization in an AGC system after deregulation," *IEEE Trans. Power Syst.*, vol. 16, no. 3, pp. 481–489, 2001.

[2] S. Bhowmik, K. Tomsovic, and A. Bose, "Communication models for third party load frequency control," *IEEE Trans. Power Syst.*, vol. 19, no. 1, pp. 543–548, 2004.

[3] K. Tomsovic, D. E. Bakken, V. Venkatasubramanian, and A. Bose, "Designing the next generation of real-time control, communication, and computations for large power systems," *Proc. IEEE*, vol. 93, no. 5, pp. 965–979, 2005.

[4] M. Liu, L. Yang, D. Gan, D. Wang, F. Gao, and Y. Chen, "The stability of AGC systems with commensurate delays," *Int. Trans. Elec. Energy Syst.*, vol. 17, no. 6, pp. 615–627, 2007.

[5] C. Peng and J. Zhang, "Delay-distribution-dependent load frequency control of power systems with probabilistic interval delays," *IEEE Trans. Power Syst.*, vol. 31, no. 4, pp. 3309–3317, 2015.

[6] P. B. Anderson, S. H. Toghroljerdi, T. M. Sørensen, B. E. Christensen, J. C. M. L. Høj, and A. Zecchino. The parker project - final report. [Online]. Available: https://parker-project.com/wp-content/uploads/2019/03/Parker_Final-report_v1.1_2019.pdf, accessed Oct 25, 2019.

[7] X. Yu and K. Tomsovic, "Application of linear matrix inequalities for load frequency control with communication delays," *IEEE Trans. Power Syst.*, vol. 19, no. 3, pp. 1508–1515, 2004.

[8] H. Bevrani, *Robust power system frequency control*. Springer, 2009.

[9] Ş. Sönmez, S. Ayasun, and U. Eminoğlu, "Computation of time delay margins for stability of a single-area load frequency control system with communication delays," *WSEAS Trans. Power Syst.*, vol. 9, pp. 67–76, 2014.

[10] Ş. Sönmez, S. Ayasun, and C. O. Nwankpa, "An exact method for computing delay margin for stability of load frequency control systems with constant communication delays," *IEEE Trans. Power Syst.*, vol. 31, no. 1, pp. 370–377, 2016.

[11] F. Milano, "Small-signal stability analysis of large power systems with inclusion of multiple delays," *IEEE Trans. Power Syst.*, vol. 31, no. 4, pp. 3257–3266, 2016.

[12] M. Liu, I. Dassios, G. Tzounas, and F. Milano, "Stability analysis of power systems with inclusion of realistic-modeling wams delays," *IEEE Trans. Power Syst.*, vol. 34, no. 1, pp. 627–636, 2019.

[13] L. Jiang, W. Yao, Q. Wu, J. Wen, and S. Cheng, "Delay-dependent stability for load frequency control with constant and time-varying delays," *IEEE Trans. Power Syst.*, vol. 27, no. 2, pp. 932–941, 2012.

[14] C.-K. Zhang, L. Jiang, Q. Wu, Y. He, and M. Wu, "Further results on delay-dependent stability of multi-area load frequency control," *IEEE Trans. Power Syst.*, vol. 28, no. 4, pp. 4465–4474, 2013.

[15] F. Yang, J. He, and D. Wang, "New stability criteria of delayed load frequency control systems via infinite-series-based inequality," *IEEE Trans. Ind. Informat.*, vol. 14, no. 1, pp. 231–240, 2018.

[16] F. Yang, J. He, and Q. Pan, "Further improvement on delay-dependent load frequency control of power systems via truncated B-L inequality," *IEEE Trans. Power Syst.*, vol. 33, no. 5, pp. 5062–5071, 2018.

[17] K. S. Ko and D. K. Sung, "The effect of EV aggregators with time-varying delays on the stability of a load frequency control system," *IEEE Trans. Power Syst.*, vol. 33, no. 1, pp. 669–680, 2018.

[18] C.-K. Zhang, L. Jiang, Q. Wu, Y. He, and M. Wu, "Delay-dependent robust load frequency control for time delay power systems," *IEEE Trans. Power Syst.*, vol. 28, no. 3, pp. 2192–2201, 2013.

[19] N. Jaleeli, L. S. VanSlyck, D. N. Ewart, L. H. Fink, and A. G. Hoffmann, "Understanding automatic generation control," *IEEE Trans. Power Syst.*, vol. 7, no. 3, pp. 1106–1122, 1992.

$$\begin{aligned}\dot{\mathcal{W}}(\eta,\chi_k) = {} & \xi^T(\eta)(\mathrm{He}(M_1^T(\gamma_k(\eta))PM_2) + e_1^TQ_1e_1 - e_3^T(Q_1-Q_2)e_3 - (1-\dot{\gamma}_k(\eta))e_2^TQ_{23}e_2 - e_4^TQ_3e_4 \\ & - \frac{1}{1-\dot{\gamma}_k(\eta)}e_5^TRe_5 + e_0^T(R+\underline{\tau}S_1+\hat{\tau}S_2)e_0 + \mathrm{He}(\Pi_1^TU_1\Pi_2 + \Pi_1^TU_2\Pi_8) + \mathrm{He}(N_0^THN_{13} + N_{12}^THN_0))\xi(\eta) \\ & + (\bar{T}_k-\eta)\xi^T(\eta)\Theta_2\xi(\eta) + \eta\xi^T(\eta)\Theta_3\xi(\eta) - \int_{-\underline{\tau}}^{0}\dot{\chi}_k^T(\eta,s)S_1\dot{\chi}_k(\eta,s)ds - \int_{-\overline{\tau}}^{-\underline{\tau}}\dot{\chi}_k^T(\eta,s)S_2\dot{\chi}_k(\eta,s)ds \\ & - \int_0^{\eta}\dot{z}^T(s)L_1\dot{z}(s)ds - \int_{\eta}^{\bar{T}_k}\dot{z}^T(s)L_2\dot{z}(s)ds. \end{aligned} \tag{21}$$

[20] J. Nanda, A. Mangla, and S. Suri, "Some new findings on automatic generation control of an interconnected hydrothermal system with conventional controllers," *IEEE Trans. Energy Convers.*, vol. 21, no. 1, pp. 187–194, 2006.

[21] P. Naghshtabrizi, J. P. Hespanha, and A. R. Teel, "Stability of delay impulsive systems with application to networked control systems," *Trans. Inst. Meas. Control*, vol. 32, no. 5, pp. 511–528, 2010.

[22] K. Liu and E. Fridman, "Wirtinger's inequality and Lyapunov-based sampled-data stabilization," *Automatica*, vol. 48, no. 1, pp. 102–108, 2012.

[23] C.-K. Zhang, Y. He, L. Jiang, M. Wu, and Q. Wu, "Stability analysis of sampled-data systems considering time delays and its application to electric power markets," *J. Franklin Inst.*, vol. 351, no. 9, pp. 4457–4478, 2014.

[24] A. Seuret, "Stability analysis of networked control systems with asynchronous sampling and input delay," in *American Control Conference (ACC)*, 2011, pp. 533–538.

[25] ——, "A novel stability analysis of linear systems under asynchronous samplings," *Automatica*, vol. 48, no. 1, pp. 177–182, 2012.

[26] K. Ramakrishnan and G. Ray, "Stability criteria for nonlinearly perturbed load frequency systems with time-delay," *IEEE Trans. Emerg. Sel. Topics Circuits Syst.*, vol. 5, no. 3, pp. 383–392, 2015.

[27] P. Kundur, *Power system stability and control*. McGraw-hill New York, 1994.

[28] C. Duan, C.-K. Zhang, L. Jiang, W. Fang, and W. Yao, "Structure-exploiting delay-dependent stability analysis applied to power system load frequency control," *IEEE Trans. Power Syst.*, vol. 32, no. 6, pp. 4528–4540, 2017.

[29] E. Fridman, A. Seuret, and J.-P. Richard, "Robust sampled-data stabilization of linear systems: an input delay approach," *Automatica*, vol. 40, no. 8, pp. 1441–1446, 2004.

[30] L. Mirkin, "Some remarks on the use of time-varying delay to model sample-and-hold circuits," *IEEE Trans. Autom. Control*, vol. 52, no. 6, pp. 1109–1112, 2007.

[31] E. Fridman, "A refined input delay approach to sampled-data control," *Automatica*, vol. 46, no. 2, pp. 421–427, 2010.

[32] Y. He, Q.-G. Wang, L. Xie, and C. Lin, "Further improvement of free-weighting matrices technique for systems with time-varying delay," *IEEE Trans. Autom. Control*, vol. 52, no. 2, pp. 293–299, 2007.

[33] H.-B. Zeng, K. L. Teo, and Y. He, "A new looped-functional for stability analysis of sampled-data systems," *Automatica*, vol. 82, pp. 328–331, 2017.

[34] L. Jin, C.-K. Zhang, Y. He, L. Jiang, and M. Wu, "Delay-dependent stability analysis of multi-area load frequency control with enhanced accuracy and computation efficiency," *IEEE Trans. Power Syst.*, 2019.

[35] Y. Zheng, G. Fantuzzi, A. Papachristodoulou, P. Goulart, and A. Wynn, "Fast ADMM for semidefinite programs with chordal sparsity," in *2017 American Control Conference (ACC)*. IEEE, 2017, pp. 3335–3340.

[36] MOSEK ApS, *MOSEK optimization toolbox for MATLAB Release 8.1.0.82*, 2019. [Online]. Available: https://docs.mosek.com/8.1/toolbox.pdf

[37] W. Tan, "Unified tuning of PID load frequency controller for power systems via IMC," *IEEE Trans. Power Syst.*, vol. 25, no. 1, pp. 341–350, 2010.

[38] A. Khalil and A. S. Peng, "Delay margin computation for load frequency control system with plug-in electric vehicles," *Int. J. Power Energy Syst.*, vol. 38, no. 3, 2018.

[39] É. Gyurkovics, "A note on Wirtinger-type integral inequalities for time-delay systems," *Automatica*, vol. 61, pp. 44–46, 2015.

[40] S. Boyd and L. Vandenberghe, *Convex optimization*. Cambridge university press, 2004.

[41] K. Liu and A. Seuret, "Comparison of bounding methods for stability analysis of systems with time-varying delays," *J. Franklin Inst.*, vol. 354, no. 7, pp. 2979–2993, 2017.

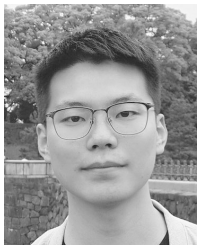

Haocheng Luo (S'18) received the B.S. degree in electrical engineering from Tsinghua University, Beijing, China, in 2015, where he is currently pursuing the Ph.D. degree. From Janunary, 2018 to January, 2019, he was a visiting Ph.D. student with the Department of Electrical Engineering and Computer Science, University of Michigan, Ann Arbor, MI, USA. His research interests include wind power generation, energy storage systems, and time-delay systems.

Ian A. Hiskens (F'06) is the Vennema Professor of Engineering in the Department of Electrical Engineering and Computer Science, University of Michigan, Ann Arbor. He has held prior appointments in the Queensland electricity supply industry, and various universities in Australia and the United States. His research interests lie at the intersection of power system analysis and systems theory, with recent activity focused largely on integration of renewable generation and controllable loads. Dr. Hiskens is involved in numerous IEEE activities in the Power and Energy Society, Control Systems Society, Circuits and Systems Society, and Smart Grid Initiative, and has served as VP-Finance of the IEEE Systems Council. He is a Fellow of IEEE and a Fellow of Engineers Australia. Dr. Hiskens is a Chartered Professional Engineer in Australia and the 2020 recipient of the M.A. Sargent Medal from Engineers Australia.

Zechun Hu (M'09–SM'17) received the B.S. and Ph.D. degrees in electrical engineering from Xian Jiao Tong University, Xian, China, in 2000 and 2006, respectively. He worked in Shanghai Jiao Tong University after graduation and also worked in University of Bath as a research officer from 2009 to 2010. He joined the Department of Electrical Engineering at Tsinghua University in 2010 where he is now an associate professor. He serves as an associate editor of IEEE Transactions on Transportation Electrification. His major research interests include optimal planning and operation of power systems, electric vehicles and energy storage systems.